- Technical Paper -

CONSIDERATION OF ASPECT RATIO IN ULTIMATE FLEXURAL LOAD-CARRYING CAPACITY OF CFS REINFORCED RC BEAM

Ming-Chien HSU [*1], Tetsukazu KIDA [*2], Tadashi ABE [*2] and Yoshitaka OZAWA [*3]

ABSTRACT

Through a series of experiments on RC beams reinforced with the carbon fiber sheet (CFS) under the static load, the authors verified the effects of the aspect ratio (ratio of beam width to depth) for RC beams reinforced with CFS. The experiments revealed that CFS can effectively reinforced RC beams, and the tensile strength of CFS is greatly influenced by the aspect ratio. The authors evaluated how the aspect ratio influences the strength of CFS; in addition, theoretical equations that proposed by authors and from CEB-FIP would be approximated with the experimental results.

Keywords: carbon fiber sheet, aspect ratio, ultimate flexural load-carrying capacity, RC beam

1. INTRODUCTION

The adhesion of carbon fiber sheet (CFS) offers various advantages such as the construction ability and the reduction of construction time. Therefore, it has been recently found in the increasing applications to the strengthening of RC member and the repair of cracked structural member. This strengthening method has been the subject of a number of studies leading to reports on suitable design methods, mechanisms and its reinforcing effects [1-7].

The present paper deals with the effects of the aspect ratio of RC beam reinforced with CFS on the beam failure mechanism. Two types of experimental specimens with different cross-sections were used. In the event of evaluating the ultimate flexural load-carrying capacity of RC beams reinforced with the CFS, the strength increasing effect of CFS is influenced greatly by the aspect ratio (that is the ratio of width (b_w) to height (h)) of RC the beams. Therefore, the authors have tried to introduce a correction factor of reinforcing effect to evaluate the effects of the aspect ratio on the strengthening effect of CFS and have proposed theoretical load-carrying capacity equations. By using the same modified and proposed method, the theoretical ultimate flexure load-carrying capacity from CEB-FIP [8] had also been modified and approximated with the experimental results.

2. PREPARATION OF EXPERIMENTAL SPECIMENS

2.1 Materials for Experimental Specimens

Ordinary Portland cement and coarse aggregate with a maximum size of 20mm were used for the experimental specimens. The D16 reinforcements of SD 295A type were used. The physical property of concrete and reinforcements

Table 1 Physical property of concrete and reinforcements

Test Specimen	Compressive strength of concrete (N/mm^2)	Reinforcements (SD295A / D16) Yield strength (N/mm^2)	Tensile strength (N/mm^2)	Young's modulus (kN/mm^2)
Type A	38.5	368	568	196
Type B	41.5			

Table 2 Physical properties of CFS

Reinforcing material	Unit weight (g/m^2)	Tensile strength (N/mm^2)	Young's modulus (kN/mm^2)
Carbon fiber	202	4420	243

are listed in Table 1. The high-strength continuous carbon fiber sheet with a width of 300mm was used, and the physical properties of CFS are listed in Table 2.

2.2 Specimen Size and Reinforcement Arrangement

Two types of RC beam specimens with different depths were prepared. The specimen sizes and the selected measuring points are shown in Fig. 1. The RC beam specimens had not reinforced with CFS and those

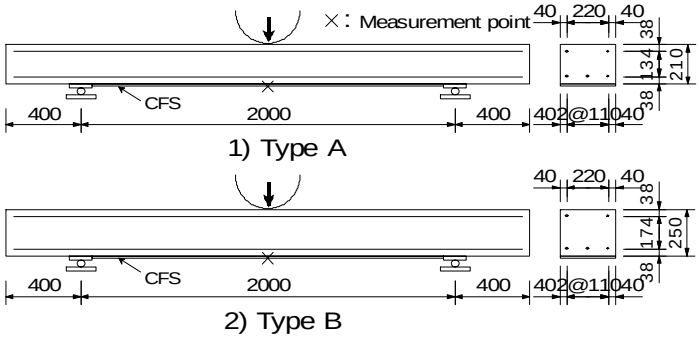

Fig. 1 Specimen size and reinforcement arrangement

*1 Assistant Professor, Dept. of Civil Engineering, College of Industrial Tech., Nihon University, Dr. E., JCI Member
*2 Professor, Dept. of Civil Engineering, College of Industrial Tech., Nihon University, Dr. E., JCI Member
*3 Associate Professor, College of Industrial Tech., Nihon University

had reinforced with CFS are referred to as "non-reinforced RC beams" and "CFS-reinforced RC beams," hereafter.
(1) Type A: It had the span of 2000mm, the width of 300mm and the height of 210mm as to the cross-section. There were three reinforcements on the tension sides with the effective depth of 172mm and two reinforcements on compression sides.
(2) Type B: It had the span and the width same as Type A, but the height was 250mm. The arrangement of the reinforcements was same as Type A, but the effective depth was 212mm.

2.3 CFS Bonding Procedures

First, the bottom surface of RC beams was ground smoothly. Then, primer and primary epoxy were applied to the bottom surface of RC beams. A single layer of CFS was then placed between two supports at the bottom of RC beams in the direction of the primary reinforcement by used the epoxy resin as an adhesive agent.

3. OUTLINE OF EXPERIMENTS

This was a flexural experiment in which a wheel was rest at the center of the span (that was at the point of maximum flexural stress). The load was increased in increments of 5.0kN by the loading controller after each experiment.

4. FAILURE MODES AND ULTIMATE FLEXURAL LOAD-CARRYING CAPACITY [9]

4.1 Failure Modes

In the flexural experiments under the static load, all non-reinforced and CFS-reinforced RC beams suffered the flexural failure as the load was being increased with cracks developing at an angle of approximately 55-60 degrees from a point directly below the wheel. The results between load and deflection show in Fig. 2. For the CFS, it peeled away from the concrete surface due to the tension at the center of the RC beam, with the peeling progressing toward the supports. Therefore, the CFS was not torn on any of the specimens; it was peeled off from the bottom of RC beams after flexural failure.

4.2 Ultimate Flexural Load-Carrying Capacity of RC Beams

(1) Non-reinforced RC Beams

The ultimate flexural load-carrying capacities were 83.0kN and 102.9kN for Types A and B, respectively. Again, all Non-reinforced RC beams failed in the flexure under the loading point.

(2) CFS-reinforced RC Beams

The ultimate flexural load-carrying capacities were 120.3kN and 137.5kN for Types A and B, respectively. Again, all CFS-reinforced RC beams also failed in flexure under the loading point.

The ultimate flexural load-carrying capacity ratios between the CFS-reinforced beam and non-reinforced RC beam subjected to static loads (CM/M; CM: CFS-reinforced RC beam; M: non-reinforced RC beam)

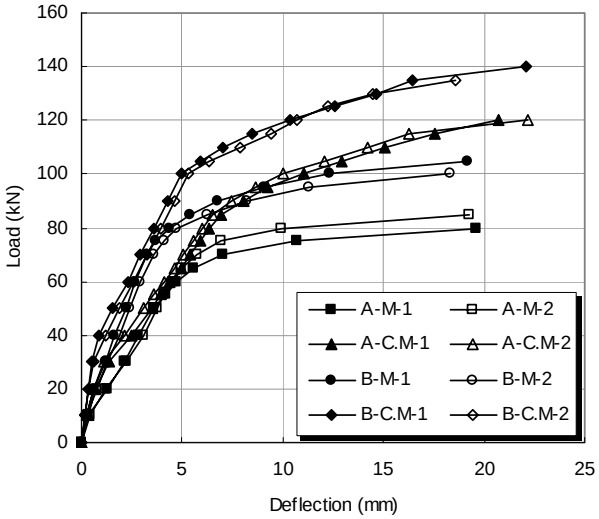

Fig.2 Relationship between load and deflection

were 1.45 and 1.34 for Types A and B, respectively, that CFS greatly improves the beam strength under static loading for both Types of RC beams.

5. COMPARISON OF THEORETICAL AND EXPERIMENTAL STRENGTH

5.1 Theoretical Ultimate Flexural Load-Carrying Capacity Equations [9]

(1) Ultimate flexural load-carrying capacity

The theoretical ultimate flexural load-carrying capacity, P_u, of the experimental beam can be calculated from the ultimate flexural load-carrying capacity equation for the rectangular cross-section with reinforcements on both tension and compression sides on the basis of the ultimate limit-state design method. The height of the equivalent stress block, a, is not larger than the thickness of the upper cover concrete for all specimen types. Accordingly, the ultimate flexural bending moment, M_u, of the specimen is given by the following Eq. 1:

$$M_u = A_s \cdot f_{yd} \cdot (d - a/2) + A_s' \cdot \sigma_s' (d' - a/2) \quad (1)$$

where,

f_{yd} is the yielding strength of reinforcement, σ_s' is the stress of compression reinforcement, A_s is the amount of reinforcement on tension side, A_s' is the amount of reinforcement on compression side, d is the effective depth, d' is the upper thickness of covering concrete, and a is the height of equivalent stress block.

The theoretical ultimate flexural load-carrying capacity, P_u, is calculated from the following Eq. 2:

$$P_u = 4 \cdot M_u / L \quad (2)$$

where,

L is the span length.

The experimental and theoretical results for the ultimate flexural load-carrying capacity of non-reinforced RC beams, derived from Eqs. 1 and 2, are shown in

Table 3 Experimental and theoretical ultimate flexural load-carrying capacities

Test Specimen		Ultimate flexural load-carrying capacity (kN)			Experimental / Theoretical
		Experimental	Theoretical		
Theoretical Equation	A-M-1	80.9	71.7	Eqs. (1) and (2)	1.13
	A-M-2	85.1			1.19
	A-C.M-1	120.9	93.1	Eqs. (3) and (2)	1.30
	A-C.M-2	119.7			1.29
	B-M-1	105.6	90.1	Eqs. (1) and (2)	1.17
	B-M-2	100.1			1.11
	B-C.M-1	139.8	113.7	Eqs. (3) and (2)	1.23
	B-C.M-2	135.1			1.19
Propose equation	A-M-1	80.9	79.6	Eqs. (4) and (2)	1.02
	A-M-2	85.1			1.07
	A-C.M-1	120.9	114.6	Eqs. (7) and (2)	1.05
	A-C.M-2	119.7			1.04
	B-M-1	105.6	100.3	Eqs. (4) and (2)	1.05
	B-M-2	100.1			1.00
	B-C.M-1	139.8	131.1	Eqs. (7) and (2)	1.07
	B-C.M-2	135.1			1.03

Table 3. A comparison of the experimental and the theoretical values for non-reinforced RC beams shows that the ratio of the experimental to the theoretical is 1.16 and 1.14 for Types A and B under the static load, respectively.

(2) Ultimate flexural bending moment of CFS-reinforced RC beams

The ultimate flexural load-carrying capacity of RC beams reinforced with the CFS has been analyzed by using many experiment results. Sakai et al. proposed Eq. 3 for the ultimate flexural load-carrying capacity when the CFS is bonded to the bottom only [11]. In this case, the theoretical ultimate flexural bending moment is calculated by using Eq. 2.

$$M_{uc}=0.90\cdot A_S\cdot f_{yd}\cdot d + 0.90\cdot A_{cs}\cdot\left(E_f/E_s\right)\cdot f_{yc}\cdot\alpha\cdot h \quad (3)$$

where,

A_{cs} is the cross-sectional area of the CFS (Table 2), E_s is the Young's modulus of reinforcement, E_f is the Young's modulus of the CFS, f_{yc} is the tensile strength of the CFS, α is the reduction factor (=1/2), and h is the height of beam.

Table 3 shows the ultimate flexural load-carrying capacities of CFS-reinforced RC beams obtained from the experimental and those derived from the theoretical equation by Sakai et al.

Comparing the experimental results and the theoretical results (derived from Eqs. 3 and 2), we see that, on average, the experimental is 1.29 times and 1.21 times larger than the theoretical for Types A and B, respectively. The reason for this relatively large discrepancy may depend on that their yield strengths as well as the tensile strength of CFS are multiplied by a reduction factor of 0.9 in Eq. 3. In additional, the reduction factor of the CFS strain at peeling is reduced by half (α=1/2), and therefore, the calculated results are on the safe side.

5.2 Proposal of the Ultimate Flexural Bending Moment Equations [9]

(1) Ultimate flexural bending moment of non-reinforced RC beams

The authors have corrected the ultimate flexural load-carrying capacity equation, taking into account the strain hardening of primary reinforcement, and proposed Eq. 4 for the ultimate flexural load-carrying capacity of beams. The theoretical equation is approximately to the values measured experimentally [9].

Ultimate flexural bending moment of non-reinforced beam under static load:

$$M_{uc}=1.13\cdot A_S\cdot f_{yd}\cdot\left(d-a/2\right) + A'_S\cdot\sigma'_S\cdot\left(d'-a/2\right) \quad (4)$$

(2) Coefficient of reinforcing effect of CFS considering aspect ratio

Proposed by Sakai et al., the tensile load-carrying capacity of the CFS is multiplied by a reduction factor α (=1/2) [11]. In the later work, Kage et al. [12] calculated the flexural load-carrying capacity of beams reinforced with the CFS by using the reduction factors α of 1/2 and 2/3 (corresponding to a peel-off area rate of 56%). From the pervious experiments [9], as the relationship between aspect ratio and coefficient of reinforcing effect in Fig. 3, coefficient of reinforcing effect varies with the type of specimen or its aspect ratio; additional, using the reduction factor as described in the reference [11 and 12] will result in variations in the ultimate flexural load-carrying capacity of beams reinforced with the CFS.

The authors have defined the ratio of the linear increase in the maximum strain to the strain at which CFS fractures as a coefficient for the reinforcing effect of CFS (β_{cf}) [9] and calculated the ultimate flexural load-carrying capacity of CFS-reinforced RC beams by multiplying the tensile load-carrying capacity of CFS by this coefficient.

$$\beta_{cfs}=\varepsilon_{ycf}/\varepsilon_y \quad (5)$$

where,

ε_{ycf} is the maximum strain of CFS, and ε_y is the fracture strain of CFS.

The reduction coefficient for CFS (β_{cfs}) [9] derived from the ratio of the maximum strain to the fracture strain of CFS (Table 2) using Eq. 5. In this case, the maximum strain of CFS from the experiments was changing as the size (width and height) of RC beam specimens was changing. Therefore, the coefficient for the reinforcing effect of CFS ($ß_{cf}$) should be consider the relationship with the ratio of beam width (b_w) to beam height (h) (the aspect ratio=b_w/h). Moreover, the relationship between the aspect ratio (b_w/h) and the coefficient for the reinforcing effect of CFS ($ß_{cf}$) is given by Eq. 6 [9].

$$\beta_{cf} = 0.57(b_w/h) - 0.15 \quad (6)$$

where,

$\beta_{cf} = 0.7$ for $\beta_{cf} > 0.7$, b_w is the width of beam, and h is the height of beam.

(3) Ultimate flexural bending moment of CFS-reinforced RC beams

The ultimate flexural load-carrying capacity of a CFS-reinforced RC beam can be calculated by adding the ultimate flexural load-capacity of CFS to the ultimate flexural load-carrying capacity of a non-reinforced RC beam derived from Eq. 7. Accordingly, the ultimate flexural bending moment of CFS-reinforced RC beam under static load can be expressed by the equation as below.

$$M_{uc} = 1.13 \cdot A_s \cdot f_{yd} \cdot (d - a/2) + A_s' \cdot \sigma_s' (d' - a/2) + 0.90 \cdot A_{cs} \cdot f_{ycf} \cdot \beta_{cf} (h - x/2) \quad (7)$$

where,

$ß_{cf}$ is from Eq. 6, A_{cs} is the cross-sectional area of CFS (Table 2), f_{ycf} is the tensile strength of the CFS, $ß_{cf}$ is the coefficient of reinforcing effect, b_w is the width of RC beam, and x is neutral axis depth.

In Eq. 7, the yield strength of the reinforcements is set to $1.13 \cdot A_s \cdot f_{yd}$ (multiplying by an increase factor of 1.13) that the specimen is an undamaged RC beam, and its strength remains after the yielding of the reinforcements due to the strain hardening. On the other hand, Sakai et al. [11] proposed using $0.90 \cdot A_s \cdot f_{yd}$ (multiplying by a reduction factor of 0.9), that the tensile reinforcements were rusted. In addition, in Eq. 7, although the coefficient for the reinforcing effect of CFS is taken into consideration, the tensile strength of CFS is set to $0.90 \cdot A_{cs} \cdot f_{ycf} \cdot ß_{cf}$ (multiplying by a reduction factor of 0.9) so that a conservative result can be obtained.

Summarizing the above, the ultimate flexural bending moment and the theoretical ultimate flexural load-carrying capacity for non-reinforced RC beam subject to static loads are calculated by Eqs.4 and 2. The ultimate flexural load-carrying capacity of a CFS-reinforced RC beam subject to static load is calculated by Eqs.7 and 2. The theoretical ultimate flexural load-carrying capacities are shown in Table 4.

5.3 Ultimate Flexural Load-Carrying Capacity for CFS-reinforced Beam from CEB-FIP [8]

(1) Ultimate flexural load-carrying capacity of non-reinforced RC beam

(a) Ultimate flexural bending moment

For calculating the ultimate load-carrying capacity, the ultimate limit state design of CEB-FIP is been used and based on the critical cross section that occurs by yielding of the tensile reinforcements followed by crushing of concrete. Accordingly, the ultimate flexural bending moment, M_{Rd}, of the specimen is given by the following Eq. 8:

$$M_{Rd} = A_s \cdot f_{yd} \cdot (d - \delta_G x) + A_s' \cdot E_s \cdot \varepsilon_s' \cdot (\delta_G x - d') \quad (8)$$

where,

$x = \dfrac{A_s f_{yd} - A_s' E_s \varepsilon_s'}{0.85 \psi f_{cd} b_w}$, $\varepsilon_s = \varepsilon_{cu} \dfrac{d - x}{x} \geq \dfrac{f_{yd}}{E_s}$,

$\varepsilon_s' = \varepsilon_{cu} \dfrac{x - d'}{x}$,

δ_G is stress block centroid coefficient (=0.4), ψ is stress block area coefficient (=0.8), f_{cd} is concrete compression strength, ε_{cu} is ultimate concrete strength, and x is neutral axis depth.

(b) Modified ultimate flexural bending moment of CEB-FIP

By looking at the results in Table 4, the experimental results are approximately 1.16 and 1.14 times of the CEB-FIP theoretical ultimate flexural load-carrying capacity for the Types A and B, respectively; there should be an adjustment for the Eq. 6 to be satisfied the experimental results. Moreover, the calculation results of theoretical equations Eq. 1 and Eq. 6 are similar and shown in Table 4. Therefore, the non-reinforced RC beam was failed around 13% times larger of the tensile reinforcements yield strength. In addition, the modified coefficient 1.13 was added into the Eq. 9 that same as Eq. 4. Furthermore, the new modified bending moment equation of CEB-FIP is showing below in Eq. 9 and results shows in Table 4.

$$M_{Rd} = 1.13 \cdot A_s \cdot f_{yd} \cdot (d - \delta_G x) + A_s' \cdot E_s \cdot \varepsilon_s' \cdot (\delta_G x - d') \quad (9)$$

Table 4 Experimental and theoretical ultimate flexural load-carrying capacities

Test Specimen		Ultimate flexural load-carrying capacity (kN)			Experimental / Theoretical
		Experimental	Theoretical		
CEB-FIP equation without adjustment coffecion	A-M-1	80.9	71.6	Eqs. (8) and (2)	1.13
	A-M-2	85.1			1.19
	A-C.M-1	120.9	107.0	Eqs. (10) and (2)	1.13
	A-C.M-2	119.7			1.12
	B-M-1	105.6	90.0	Eqs. (8) and (2)	1.17
	B-M-2	100.1			1.11
	B-C.M-1	139.8	145.0	Eqs. (10) and (2)	0.96
	B-C.M-2	135.1			0.93
CEB-FIP equation with adjustment coffecion	A-M-1	80.9	80.7	Eqs. (9) and (2)	1.00
	A-M-2	85.1			1.05
	A-C.M-1	120.9	102.8	Eqs. (11) and (2)	1.18
	A-C.M-2	119.7			1.16
	B-M-1	105.6	101.3	Eqs. (9) and (2)	1.04
	B-M-2	100.1			0.99
	B-C.M-1	139.8	128.5	Eqs. (11) and (2)	1.09
	B-C.M-2	135.1			1.05

(2) Ultimate flexural bending moment of CFS-reinforced RC beams

(a) Ultimate flexural bending moment

The ultimate limit state design of CEB-FIP is based on the critical cross section that occurs by yielding of the tensile reinforcements followed by crushing of concrete. Fig. 4 [8] shows the design bending moment of the strengthened cross section that based on principles of RC design. Eq. 10 is the design ultimate flexural bending moment capacity.

$$M_{Rd} = A_S \cdot f_{yd} \cdot (d - \delta_G x) + A_S' \cdot E_S \cdot \varepsilon_S' \cdot (\delta_G x - d') + A_{CS} \cdot E_f \cdot \varepsilon_f \cdot (h - \delta_G x) \quad (10)$$

where,

$x = \dfrac{A_S f_{yd} + A_{CS} E_f \varepsilon_f - A_S' E_S \varepsilon_S'}{0.85\psi f_{cd} b_W}$,

$\varepsilon_f = \varepsilon_{cu} \dfrac{h-x}{x} - \varepsilon_o \le \varepsilon_y$, ε_f is the strain of CFS, and ε_o is initial strain of concrete.

In the Eq. 10, the strain of CFS is been calculated related to the ultimate concrete strain, the high of RC beam, the neutral axle, and the initial strain of concrete. This means that the full strain of CFS was not been considered into the calculation since the concrete had been taken some initial strain into the consideration. Moreover, the stress distribution for calculating the neutral axle in the Eq. 10 had considered the stress of CFS. Therefore, the ratios between the experimental and the CEB-FIP theoretical results are approximately 1.13 and 0.95 for the Types A and B, respectively.

(b) Modified ultimate flexural load-carrying capacity for CEB-FIP

The Eq. 11 had been modified by using the same concept of Eq. 7. The 1.13 coefficient was added because of the results are shown in Table 3 that the failure of non-reinforced RC beams was approximately 13% larger than the yield strength of tensile reinforcement. The aspect ratio β_{cf} was been added into the CFS calculation to showing the size effect in the calculation. The new CEB-FIP modified design bending moment for calculating CFS-reinforced RC beam is written below.

$$M_{Rd} = 1.13 \cdot A_S \cdot f_{yd} \cdot (d - \delta_G x) + A_S' \cdot E_S \cdot \varepsilon_S' \cdot (\delta_G x - d') + A_{CS} \cdot E_f \cdot \varepsilon_f \cdot \beta_{cf} \cdot (h - \delta_G x) \quad (11)$$

Summarizing the above, the ultimate flexural load-carrying capacity for non-reinforced RC beams under the static load is calculated by Eqs. 8 and 2; Eqs.10 and 2 are for CFS-reinforced RC beams before the modification of CEB-FIP equations. After the modification of CEB-FIP equations, the ultimate flexural load-carrying capacity under the static load is calculated by Eqs. 9 and 2 for non-reinforced RC beams; Eqs. 11 and 2 for CFS-reinforced RC beams. The calculation results compared with the experimental results are shown in Table 4.

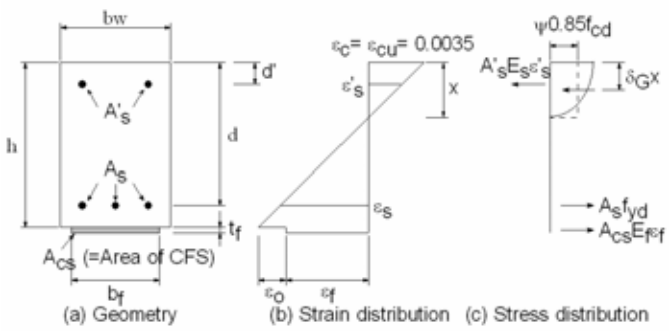

Fig. 4 Cross section of maximum limit state in bending

5.4 Comparison between Experimental and Theoretical Results

(1) Non-reinforced RC Beams

(a) Proposed the modified theoretical equation

In Table 3, the theoretical ultimate flexural load-carrying capacity of RC beams without CFS reinforcement under the static load is calculated by using Eqs. 4 and 2, that given a ratio of approximately 1.04 and 1.03 times of the theoretical ultimate flexural load-carrying capacity for the Types A and B, respectively.

(b) The modified CEB-FIP theoretical equation

Comparing the results of the experimental and the modified CEB-FIP in Table 4, the ratio of ultimate flexural load-carrying capacities is approximately 1.03 and 1.02 times of the theoretical ultimate flexural load-carrying capacity (Eqs. 9 and 2) for the Types A and B, respectively. Therefore, the modified coefficient 1.13 should be suitable to add into the theoretical ultimate flexural bending moment calculation of CEB-FIP for the non-reinforced RC beam.

(2) CFS-reinforced RC Beams

(a) Proposed the modified theoretical equation

In Table 3, the ultimate flexural load-carrying capacity of specimens reinforced with CFS under the static load is calculated by using Eqs. 7 and 2 with the reinforcing effect coefficient obtained in the present paper. The experimental ultimate flexural load-carrying capacities are approximately 1.05 and 1.02 times of the theoretical values for the Types A and B, respectively.

(b) Modified CEB-FIP theoretical equation

Comparing the results of the experimental and the modified CEB-FIP in Table 4, the ratio of ultimate flexural load-carrying capacities is approximately 1.17 and 1.07 times of the theoretical values (Eqs. 11 and 2) for the Types A and B, respectively.

The ultimate flexural load-carrying capacity of CEB-FIP for CFS-reinforced RC beam was considered the strength of CFS in the neutral axis and strain of CFS with the initial strain of concrete at bottom of strain distribution as shown in Fig. 2. It was different from the proposed equation by the authors just adding the ultimate flexural load-carrying capacity of CFS into the ultimate flexural load-carrying capacity of the non-reinforced RC beam.

6. CONCLUSIONS

(1) The failure modes of RC beams reinforced with the CFS under the static load were the flexural failure for the Types A and B. In any case, the fracture failure was never occurred to the CFS that peeled away from the concrete surface by virtue of the tensile stresses at the center of the RC beam.

(2) The ultimate flexural load-carrying capacity for the CFS reinforcing effect on RC beams was 45% and 34% higher for the Types A and B, respectively, than the non-reinforced RC beams. These results indicate that the ultimate flexural load-carrying capacity varies with the aspect ratio of beam.

(3) The tensile load-carrying capacity of CFS, which is required to calculate the ultimate flexural load-carrying capacity of the RC beam reinforced with CFS, is affected greatly by the aspect ratio (b_w /h) of the beam. Thus, the authors have proposed the coefficient of reinforcing effect of CFS as a function of the aspect ratio.

(4) It has been verified that the general ultimate flexural load-carrying capacity equation of RC beam reinforced with the CFS can be well evaluated by using a coefficient of reinforcing effect (β_{cf}) proposed by this paper. In the condition of that the ultimate flexural load-carrying capacity of CFS was added into the ultimate flexural load-carrying capacity of the non-reinforced RC beam.

(5) For non-reinforced RC beam, the ultimate flexural load-carrying capacity of CEB-FIP could be modified to the experimental by adding the coefficient as the modified equation proposed by the authors.

(6) For CFS-reinforced RC beam, the ultimate load-carrying capacity of CEB-FIP had considered stress of CFS while calculated the neutral axle. Also, the strain of CFS was not fully considered into the ultimate load-carrying capacity calculation. Moreover, it was related to the ultimate concrete strain, the high of RC beam, the neutral axle, and the initial strain of concrete. In additional, the CFE-FIP calculation had already considered the high of RC beam while calculating the CFS strain (ε_f) and the width of RC beam while calculating the neutral axle of RC beam. Therefore, the coefficient for the reinforcing effect of CFS (β_{cf}) is not necessary to be added into the CEB-FIP calculation for CFS-reinforced RC beam.

ACKNOWLEDGEMENT

The authors acknowledge for the materials supporting from NCK Co., Ltd (CFS) and SHO-BOND Co., Ltd (repairing crack's materials).

REFERENCES

[1] Takahashi, Y., Hata, C., Maeda, T., and Sato, Y., "Experimental Study of Flexural Behavior of Aramid FRP Rods Reinforced Concrete Beam with Externally Bonded Carbon Fiber Sheet", Proceedings of the Japan Concrete Institute, Vol.20, No.1, pp. 509-514, 1998

[2] Mikami, H., Kishi, N., Sato, M., and Kurihashi, Y., "Effect of Strengthened Area on Bending Capacity of RC Beams Adhered with FRP Sheet", Proceedings of the Japan Concrete Institute, Vol. 21, No.3, pp. 1549-1554, 1999

[3] Kurihashi, Y., Kishi, N., Mikami, H., and Matsuoka, K., "Flexural Bonding Property of FRP Sheet on RC Beam with Two-point Loading", Proceedings of the Japan Concrete Institute, Vol. 21, No.3, pp. 1555-1560, 1999

[4] Anania, L., Badala, A., and Failla, G., "Increasing the Flexural Performance of RC Beams Strengthened with CFRP Materials", Construction and Building Materials, pp.55-61, 2005

[5] Oh, H., Sim, J., and Meyer, C., "Experimental Assessment of Bridge Deck Panels Strengthened with Carbon Fiber Sheets", Composites Part B: Engineering, Vol.34, Issue 6, pp.527-538, 2003

[6] Lee, J.K. and Lee, J.H., "Nondestructive Evaluation on Damage of Carbon Fiber Sheet Reinforced Concrete", Composite Structures, Vol. 58, Issue 1, pp.139-147, 2002

[7] Takeda, K., Mitsui, U, Murakami, K., Sakai, H., and Nakamura, M., "Flexural Behaviour of Reinforced Concrete Beams Strengthened with Carbon Fibre Sheets", Composites Part A: Applied Science and Manufacturing, Vol. 27, Issue 10, pp. 981-987, 1996

[8] "Externally bonded FRP reinforcement for RC structures", CEB-FIP, pp.34-36, 2001

[9] Hsu, M.C., Abe, T., Kida, T., Sawano, T., and Minakuchi, K., "Reinforcing Effects and Mechanical Properties of RC Beam with CFS under Static and Running Loads", Journal of Marine Science and Technology, Vol. 14, No.2, pp. 73-83, 2006

[10] Abe, T., Kida, T., Sawano, T., Hoshino, M., and Kato, K., "Flexural Load-Carrying Capacity and Failure Mechanism of RC Beams with Low Effective Depth under Running Wheel-Load", Materials Science Research International, Vol.7, No.3, pp. 186-193, 2001

[11] Sakai, H., Tomosawa, F., Masuda, Y., Abe, M., Noguchi, T., Kage, T., Lee, H.S., and Hisabe, N., "CFRP Sheet Strengthening of Reinforced Concrete Members Damaged by Rebar Corrosion", Summaries of Technical Papers of Annual Meeting Architectural Institute of Japan, A-1, Materials and construction pp. 345-346, 1996

[12] Kage, T. and Masuda, Y., "Influence of Separation on Flexural Performance of RC Beam reinforced by CFRP-Sheets", Proceedings of the Japan Concrete Institute, Vol.20, No.1, pp.425-430, 1998